

# Magnetic monopole condensation in pyrochlore ice quantum spin liquid: application to $\text{Pr}_2\text{Ir}_2\text{O}_7$ and $\text{Yb}_2\text{Ti}_2\text{O}_7$

Gang Chen<sup>1,2</sup>

<sup>1</sup>*State Key Laboratory of Surface Physics, Center for Field Theory and Particle Physics,  
Department of Physics, Fudan University, Shanghai 200433, China and*

<sup>2</sup>*Collaborative Innovation Center of Advanced Microstructures, Fudan University, Shanghai, 200433, China*  
(Dated: May 10, 2016)

Pyrochlore iridates and pyrochlore ices are two families of materials where novel quantum phenomena are intertwined with strong spin-orbit coupling, substantial electron correlation and geometrical frustration. Motivated by the puzzling experiments on two pyrochlore systems  $\text{Pr}_2\text{Ir}_2\text{O}_7$  and  $\text{Yb}_2\text{Ti}_2\text{O}_7$ , we study the proximate Ising orders and the quantum phase transition out of quantum spin ice U(1) quantum spin liquid (QSL). We apply the electromagnetic duality of the compact quantum electrodynamics to analyze the “magnetic monopoles” condensation for U(1) QSL. The monopole condensation transition represents a unconventional quantum criticality with unusual scaling laws. It naturally leads to the Ising orders that belong to the “2-in 2-out” spin ice manifold and generically have an enlarged magnetic unit cell. We demonstrate that the antiferromagnetic Ising state with the ordering wavevector  $\mathbf{Q} = 2\pi(001)$  is proximate to U(1) QSL while the ferromagnetic Ising state with  $\mathbf{Q} = (000)$  is not proximate to U(1) QSL. This implies that if there exists a direct transition from U(1) QSL to the ferromagnetic Ising state, the transition must be strongly first order. We apply the theory to  $\text{Pr}_2\text{Ir}_2\text{O}_7$  and  $\text{Yb}_2\text{Ti}_2\text{O}_7$ .

Pyrochlore iridates ( $\text{R}_2\text{Ir}_2\text{O}_7$ )<sup>1,2</sup> have stimulated a wide interest in recent years, and many interesting results, including topological Mott insulator<sup>3</sup>, quadratic band touching<sup>4</sup>, Weyl semimetal<sup>5–7</sup>, non-Fermi liquid<sup>8,9</sup> and so on, have been proposed. Among these materials,  $\text{Pr}_2\text{Ir}_2\text{O}_7$  is of particular interest. In  $\text{Pr}_2\text{Ir}_2\text{O}_7$ , the Ir system remains metallic at low temperatures<sup>10</sup>. More intriguingly, no magnetic order was found except a partial spin freezing of the Pr moments due to disorder at very low temperatures in the early experiments<sup>10–12</sup>. A recent experiment on different  $\text{Pr}_2\text{Ir}_2\text{O}_7$  samples, however, discovered an antiferromagnetic long-range order for the Pr moments<sup>13</sup>. While most theory works on pyrochlore iridates focused on the Ir pyrochlores and explored the interplay between the electron correlation and the strong spin-orbit coupling of the Ir 5d electrons<sup>3,14,15</sup>, very few works considered the influence and the physics of the local moments from the rare-earth sites that also form a pyrochlore lattice<sup>7,16–18</sup>. In this paper, we address the local moment physics in  $\text{Pr}_2\text{Ir}_2\text{O}_7$  and propose that the disordered state of the Pr moments is likely to be in the quantum spin ice (QSI) U(1) quantum spin liquid state. We explore the proximate Ising order and the confinement transition of QSI and argue that  $\text{Pr}_2\text{Ir}_2\text{O}_7$  could be located near such a confinement transition.

The QSI U(1) QSL is an exotic quantum phase of matter and is described by emergent compact quantum electrodynamics, or equivalently, by the compact U(1) lattice gauge theory (LGT) with a gapless U(1) gauge photon and deconfined spinon excitations<sup>19–21</sup>. Recently several rare-earth pyrochlores with 4f electron local moments are proposed as candidates for QSI U(1) QSLs<sup>22–32</sup>. In these systems, the predominant antiferromagnetic exchange interaction between the Ising components of the local moments favors an extensively degenerate “2-in 2-out” spin ice manifold on the pyrochlore lattice<sup>20,22,33–37</sup>. The

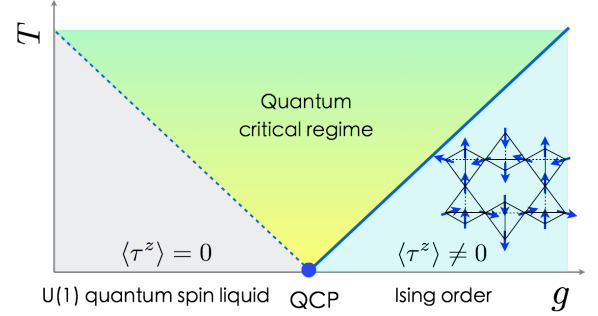


FIG. 1. The monopole condensation transition from the QSI U(1) QSL to the proximate antiferromagnetic Ising state. The dashed (solid) line represents a thermal crossover (transition). “ $g$ ” is a tuning parameter that corresponds to the mass of “magnetic monopole” (see the discussion in the main text). The inset Ising order has an ordering wavevector  $\mathbf{Q} = 2\pi(001)$ . The Pr moment of  $\text{Pr}_2\text{Ir}_2\text{O}_7$  is likely to be close to this quantum critical point (QCP).

transverse spin interaction allows the system to tunnel quantum mechanically within the ice manifold, giving rise to a U(1) QSL ground state<sup>36–41</sup>. Like  $\text{Pr}_2\text{Ir}_2\text{O}_7$ , the experimental results on these QSL candidate materials depend sensitively on the stoichiometry and the sample preparation<sup>22</sup>. In particular, for the pyrochlore ice system  $\text{Yb}_2\text{Ti}_2\text{O}_7$ , while some samples remain disordered down to the lowest temperature and the neutron scattering shows a diffusive scattering<sup>23,42</sup>, others develop a ferromagnetic order<sup>25,43–45</sup>. This suggests that both the Yb moments in  $\text{Yb}_2\text{Ti}_2\text{O}_7$  and the Pr moments in  $\text{Pr}_2\text{Ir}_2\text{O}_7$  could be located near a phase transition between a disordered state (that might be a QSI U(1) QSL) and the magnetic orders.

On the theoretical side, the instability of the QSI U(1)

QSL and the proximate magnetic orders have not been fully explored. The early works based on the gauge mean-field approach studied the instability by spinon condensation. The spinon condensation transition, known as “Anderson-Higgs transition”, generically leads to the transverse spin order that is not in the spin ice manifold<sup>38</sup>. Instead, we here study the proximate Ising spin order and transition out of QSI U(1) QSL by condensing the “magnetic monopoles” that are topological excitations of the compact U(1) LGT for the U(1) QSL<sup>46</sup>. The monopole condensation transition is the *confinement transition* of the compact U(1) LGT<sup>47,48</sup>, and the resulting proximate Ising order is in the ice manifold and generically breaks the translation symmetry. We determine the structure of the proximate Ising orders of the QSI U(1) QSL and explain the nature of the phase transition from the QSI U(1) QSL to the Ising orders.

### Results.

**Compact QED and electromagnetic duality.** Even though more complicated realistic Hamiltonians are available for effective spin-1/2 moments on the pyrochlore lattice<sup>39–41</sup>, it is known that the spin-1/2 XXZ model<sup>19</sup>,

$$H = \sum_{\langle ij \rangle} [J_z \tau_i^z \tau_j^z - J_\perp (\tau_i^+ \tau_j^- + \tau_i^- \tau_j^+)], \quad (1)$$

in the perturbative regime ( $|J_\perp|/J_z \ll 1$ ) already captures the *universal* properties of the QSI U(1) QSL. Here  $J_z > 0$ ,  $\tau_i^\pm \equiv \tau_i^x \pm i\tau_i^y$ , and  $\tau_i^z$  is defined along the local  $\langle 111 \rangle$  direction of each pyrochlore site. In the perturbative regime, the third order degenerate perturbation yields a ring exchange model<sup>19</sup>,

$$H_{\text{ring}} = - \sum_{\odot_p} \frac{K}{2} (\tau_1^+ \tau_2^- \tau_3^+ \tau_4^- \tau_5^+ \tau_6^- + h.c.), \quad (2)$$

where  $K = 24J_\perp^3/J_z^2$  and “1, ..., 6” are 6 sites on the perimeter of the elementary hexagons (“ $\odot_p$ ”) of the pyrochlore lattice.

To map the ring exchange model to the compact U(1) LGT, one introduces the lattice vector gauge fields as<sup>19</sup>

$$E_{\mathbf{r}\mathbf{r}'} \equiv \tau_i^z + \frac{1}{2}, \quad (3)$$

$$e^{\pm i A_{\mathbf{r}\mathbf{r}'}} \equiv \tau_i^\pm, \quad (4)$$

where the pyrochlore site  $i$  resides on the center of the nearest-neighbor diamond link  $\langle \mathbf{r}\mathbf{r}' \rangle$ , and  $\mathbf{r}$  ( $\mathbf{r}'$ ) is on the I (II) sublattice of the diamond lattice that is formed by the centers of the tetrahedra. Moreover,  $E_{\mathbf{r}\mathbf{r}'} = -E_{\mathbf{r}'\mathbf{r}}$ ,  $A_{\mathbf{r}\mathbf{r}'} = -A_{\mathbf{r}'\mathbf{r}}$  and  $[E_{\mathbf{r}\mathbf{r}'}, A_{\mathbf{r}\mathbf{r}'}] = i$ . Here  $E_{\mathbf{r}\mathbf{r}'}$  ( $A_{\mathbf{r}\mathbf{r}'}$ ) is integer valued ( $2\pi$  periodic). With this transformation,  $H_{\text{ring}}$  is transformed into the compact U(1) LGT on the diamond lattice formed by the centers of the tetrahedra,

$$H_{\text{LGT}} = \sum_{\langle \mathbf{r}\mathbf{r}' \rangle} \frac{U}{2} (E_{\mathbf{r}\mathbf{r}'} - \frac{\epsilon_{\mathbf{r}}}{2})^2 - \sum_{\odot_d} K \cos(\text{curl } A), \quad (5)$$

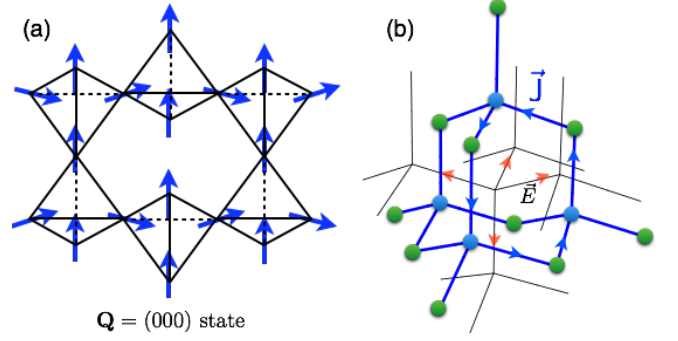


FIG. 2. (a) The  $\mathbf{Q} = (000)$  ferromagnetic state. (b) The diamond lattice (in thin black) and the dual diamond lattice (in thick blue). The monopole loop current ( $\vec{J}$ ) on the hexagon of the dual diamond lattice gives rise to the electric field ( $\vec{E}$ ) on the link of the diamond lattice via the right hand's rule.

where we have added the electric field term with the stiffness  $U$ ,  $\epsilon_{\mathbf{r}} = +1(-1)$  for  $\mathbf{r} \in \text{I (II)}$  sublattice, and the lattice curl ( $\text{curl } A \equiv \sum_{\mathbf{r}\mathbf{r}' \in \odot_d} A_{\mathbf{r}\mathbf{r}'}$ ) defines the internal magnetic field  $B$  through the center of the diamond hexagon ( $\odot_d$ ). In the large  $U$  limit, the microscopic  $\tau^z = \pm 1/2$  is recovered. Although the actual values of  $U$  and  $K$  in the low energy description of U(1) QSL are renormalized from the perturbative results,  $H_{\text{LGT}}$ , that captures the universal properties of U(1) QSI QSL<sup>19</sup>, is the starting point of our analysis below.

“Magnetic monopoles” are topological defects of the U(1) gauge field and carry the magnetic charge. To describe the magnetic transition from U(1) QSL via the monopole condensation, it is inconvenient to work with the field variables in Eq. (5) because the monopole variable is not explicit<sup>19</sup>. Instead, we apply the electromagnetic duality<sup>19,48–53</sup> to reformulate the compact U(1) LGT Hamiltonian and make the monopole explicit. We first introduce an integer-valued dual U(1) gauge field  $a_{\mathbf{r}\mathbf{r}'}$  that lives on the link of the dual diamond lattice (see Fig. 2b) such that

$$\text{curl } a \equiv \sum_{\mathbf{r}\mathbf{r}' \in \odot_d^*} a_{\mathbf{r}\mathbf{r}'} \equiv E_{\mathbf{r}\mathbf{r}'} - E_{\mathbf{r}\mathbf{r}'}^0, \quad (6)$$

where “ $\odot_d^*$ ” refers to the elementary hexagon on the dual honeycomb lattice and the electric field vector  $E_{\mathbf{r}\mathbf{r}'}$  penetrates through the center of “ $\odot_d^*$ ”. Here the serif symbols  $\mathbf{r}, \mathbf{r}'$  label the dual diamond lattice sites. We have introduced a background electric field distribution  $E_{\mathbf{r}\mathbf{r}'}^0$  that takes care of the background charge distribution due to the “2-in 2-out” ice rule. Each state in the spin ice manifold corresponds to a background electric field distribution. For our convenience, we choose a simple electric field configuration that corresponds to a uniform “2-in 2-out” spin ice state (see Fig. 2a) with

$$E_{\mathbf{r}, \mathbf{r} + \epsilon_{\mathbf{r}} \mathbf{e}_0}^0 = E_{\mathbf{r}, \mathbf{r} + \epsilon_{\mathbf{r}} \mathbf{e}_1}^0 = \epsilon_{\mathbf{r}}, \quad (7)$$

$$E_{\mathbf{r}, \mathbf{r} + \epsilon_{\mathbf{r}} \mathbf{e}_2}^0 = E_{\mathbf{r}, \mathbf{r} + \epsilon_{\mathbf{r}} \mathbf{e}_3}^0 = 0, \quad (8)$$

where  $\mathbf{e}_\mu$  ( $\mu = 0, 1, 2, 3$ ) are the four vectors that connect the I sublattice sites of the diamond lattice to their nearest neighbors. In terms of the dual gauge variables,  $H_{\text{LGT}}$  is transformed into

$$H_{\text{dual}} = \sum_{\mathbf{O}_d^*} \frac{U}{2} (\text{curl } a - \bar{E})^2 - \sum_{\langle \mathbf{r}, \mathbf{r}' \rangle} K \cos B_{\mathbf{r}\mathbf{r}'}, \quad (9)$$

where we have explicitly replaced  $\text{curl } A$  with the magnetic field vector  $B_{\mathbf{r}\mathbf{r}'}$  that lives on the link  $\langle \mathbf{r}\mathbf{r}' \rangle$  of the dual diamond lattice and is conjugate to the dual gauge field  $a$  with  $[B_{\mathbf{r}\mathbf{r}'}, a_{\mathbf{r}\mathbf{r}'}] = i$ . In Eq. (9), we have introduced the electric field  $\bar{E}$  that combines both the background electric field distribution  $E^0$  and the offset in Eq. (5) with

$$\bar{E}_{\mathbf{r}, \mathbf{r} + \epsilon_{\mathbf{r}} \mathbf{e}_\mu} = E_{\mathbf{r}, \mathbf{r} + \epsilon_{\mathbf{r}} \mathbf{e}_\mu}^0 - \frac{\epsilon_{\mathbf{r}}}{2}. \quad (10)$$

Since the dual gauge field  $a$  is integer valued, the dual Hamiltonian  $H_{\text{dual}}$  is difficult to work with. Moreover, the “magnetic monopole” is implicit in the dual gauge field configuration. To make the monopole explicit, we follow the standard procedure<sup>19</sup>, first relax the integer valued constraint of the dual gauge field by introducing  $\cos 2\pi a$  and then insert the monopole operators. The resulting dual theory is described by the magnetic monopoles minimally coupled with the dual U(1) gauge field on the dual diamond lattice,

$$H_{\text{dual}} = \sum_{\mathbf{O}_d^*} \frac{U}{2} (\text{curl } a - \bar{E})^2 - \sum_{\mathbf{r}, \mathbf{r}'} K \cos B_{\mathbf{r}\mathbf{r}'} - \sum_{\langle \mathbf{r}, \mathbf{r}' \rangle} t \cos(\theta_{\mathbf{r}} - \theta_{\mathbf{r}'} + 2\pi a_{\mathbf{r}\mathbf{r}'}), \quad (11)$$

where  $e^{-i\theta_{\mathbf{r}}}$  ( $e^{i\theta_{\mathbf{r}}}$ ) creates (annihilates) the “magnetic monopole” at the dual lattice site  $\mathbf{r}$ .

**Monopole condensation and proximate Ising order.** In the dual gauge Hamiltonian of Eq. (11), as the monopole hopping increases, the monopole gap decreases. When the monopole gap is closed, the monopole is condensed. In the confinement phase, the  $E$  field develops a static distribution, the  $B$  field (the  $a$  field) is strongly (weakly) fluctuating. Therefore, it is legitimate to first ignore the  $a$  field fluctuation, then study the monopole band structure, and condense the monopoles at the minimum of the monopole band for the confinement phase<sup>51,52</sup>. In such a dual gauge mean-field-like treatment, the “ $U$ ” term in the Hamiltonian enforces  $\text{curl } \bar{a} = \bar{E}$ , which is solved to fix the gauge for the dual gauge field. Here we set the dual gauge field to its static component  $\bar{a}$ . The electric field distribution  $\bar{E}$  turns into the dual gauge flux experienced by the “magnetic monopoles” in the dual formulation. As  $\bar{E}$  takes  $\pm \epsilon_{\mathbf{r}}/2$ , it leads to  $\pi$  flux of the dual gauge field through each elementary hexagon on the dual diamond lattice. As it is shown in Fig. 3, we fix the gauge by setting  $\bar{a}_{\mathbf{r}, \mathbf{r} + \mathbf{e}_\mu} = \xi_\mu(\mathbf{q} \cdot \mathbf{r})$ , where  $\mathbf{r} \in \text{I sublattice}$  of the dual diamond lattice,  $\mathbf{e}_\mu$  ( $\mu = 0, 1, 2, 3$ ) refer to the four nearest-neighbor vectors of the dual diamond lattice,  $(\xi_0, \xi_1, \xi_2, \xi_3) = (0110)$  and  $\mathbf{q} = 2\pi(100)$ .

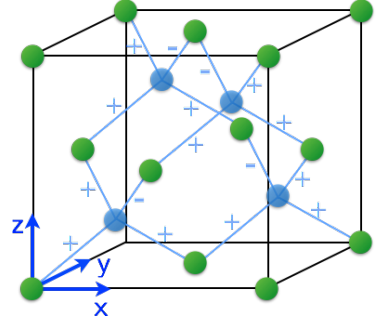


FIG. 3. The dual diamond lattice and the assignment of the gauge potential  $e^{-i2\pi\bar{a}_{\mathbf{r}\mathbf{r}'}}$  on the nearest neighbor links.

In the presence of the background flux, the monopole nearest-neighbor hopping model on the dual diamond lattice is given by

$$H_m = - \sum_{\langle \mathbf{r}, \mathbf{r}' \rangle} t e^{-i2\pi\bar{a}_{\mathbf{r}\mathbf{r}'}} \Phi_{\mathbf{r}}^\dagger \Phi_{\mathbf{r}'}, \quad (12)$$

where we have introduced  $\Phi_{\mathbf{r}} \equiv e^{i\theta_{\mathbf{r}}}$  (with  $|\Phi_{\mathbf{r}}| \equiv 1$ ). The dispersion of the lowest monopole band is given by

$$\Omega_{\mathbf{k}} = -|t| [4 + 2(3 + c_x c_y - c_x c_z + c_y c_z)^{1/2}]^{1/2}, \quad (13)$$

where  $c_\mu = \cos k_\mu$  ( $\mu = x, y, z$ ). The degenerate minima of the lowest band form several lines of momentum points in the Brillouin zone. One such degenerate line is along the [001] direction of the Brillouin zone and the minimum energy is  $-2\sqrt{2}|t|$ . Other degenerate lines are readily obtained by the symmetry operations. The line degeneracy of the band minima is a consequence of the background flux that frustrates the monopole hopping. These continuous degeneracies are accidental and are not protected by symmetry. It is expected that the further neighbor monopole hopping or monopole interactions should lift these degeneracies.

Because of the background flux, the lattice symmetry in  $H_m$  is realized projectively, known as projective symmetry group (PSG)<sup>54</sup>. We use PSG to generate the further neighbor monopole hoppings<sup>55</sup>, but do not find obvious degeneracy breaking. Instead, the line degeneracy immediately gets lifted if we impose the unimodular constraint of the monopole field ( $|\Phi_{\mathbf{r}}| = 1$ ). This unimodular constraint, that originates from the repulsive interaction between monopoles, suppresses the magnitude fluctuation of the monopole fields. For the degenerate minima along the [001] direction, the unimodular requirement selects the monopole configurations at two equivalent momenta

$$\mathbf{k}_1 = (0, 0, \pi), \quad \mathbf{k}_2 = (0, 0, -\pi), \quad (14)$$

and the corresponding monopole configurations are

$$\begin{cases} \mathbf{r} \in \text{I}, & \varphi_1(\mathbf{r}) = (\frac{1+i}{2} + \frac{1-i}{2} e^{i2\pi x}) e^{i\pi z}, \\ \mathbf{r} \in \text{II}, & \varphi_1(\mathbf{r}) = e^{i\pi z}, \end{cases} \quad (15)$$

$$\begin{cases} \mathbf{r} \in \text{I}, & \varphi_2(\mathbf{r}) = (\frac{i+1}{2} + \frac{i-1}{2} e^{i2\pi x}) e^{-i\pi z}, \\ \mathbf{r} \in \text{II}, & \varphi_2(\mathbf{r}) = i e^{-i\pi z}, \end{cases} \quad (16)$$

where  $\varphi_a$  refers to the monopole configuration at the momentum  $\mathbf{k}_a$ . From the above results, we use the PSG transformations and generate in total twelve symmetry equivalent solutions.

After the unimodular constraint is enforced, the monopoles are condensed at only one of the equivalent solutions, the spinons are confined and the system develops an Ising order. Although the Ising order is induced by the monopole condensation, as monopoles are emergent particles and are not gauge invariant, the physical property of the monopole condensate is encoded in the gauge invariant monopole bilinears. Again, symmetry is a powerful tool to establish the relation between the spin density  $\tau^z$  and the monopole bilinears. The candidate monopole bilinears are the monopole density and the monopole current. Although the monopole density ( $\Phi^\dagger\Phi$ ) transforms in the same way as the spin density ( $\tau^z$ ) under the space group symmetry, they behave oppositely under the time reversal.

As for the monopole current, from the Maxwell's equations, the loop integral of monopole current is the electric flux through the plaquette enclosed by the loop (see Fig. 2b)<sup>51,52</sup>. We have

$$\tau_i^z \sim E_{\mathbf{r}\mathbf{r}'} \sim \sum_{\mathbf{r}\mathbf{r}' \in \odot_d^*} \mathbf{J}_{\mathbf{r}\mathbf{r}'}, \quad (17)$$

where the pyrochlore site  $i$  is the center of the elementary honeycomb  $\odot_d^*$  on the dual diamond lattice, and  $\mathbf{J}_{\mathbf{r}\mathbf{r}'} \equiv i(\langle \Phi_{\mathbf{r}}^\dagger \rangle \langle \Phi_{\mathbf{r}'} \rangle e^{-i\tilde{a}_{\mathbf{r}\mathbf{r}'}} - h.c.)$  defines the monopole current. Here  $\langle \Phi_{\mathbf{r}} \rangle$  is the expectation value of the monopole field that is taken with respect to one of the equivalent solutions. In the inset of Fig. 1, we depict the spin density distribution of the monopole condensate at  $\mathbf{k}_1$ . The resulting Ising order in the confinement phase is an antiferromagnetic state with an ordering wavevector  $\mathbf{Q} = 2\pi(001)$ , and the four spins on each tetrahedron obey the “2-in 2-out” ice rule. This Ising state breaks the translation symmetry by doubling the crystal unit cell.

The translation symmetry breaking of the proximate magnetic state is a generic phenomenon. The background gauge flux, due to the “2-in 2-out” rule, shifts the minimum of the monopole band to finite momenta. Once the monopole is condensed at the finite momentum, the resulting proximate Ising order necessarily breaks the translation symmetry. If, however, the ferromagnetic Ising order with  $\mathbf{Q} = (000)$  in Fig. 2a, preserves the translation symmetry and borders with the QSI U(1) QSL, the transition between this ferromagnetic Ising order and U(1) QSL must be strongly first order. In the Method, we write down simple models that do not have a sign problem for quantum Monte Carlo simulation. The models can realize both the ferromagnetic and antiferromagnetic Ising orders and allow the careful numerical study of the phase transitions out of the QSI U(1) QSL.

**Critical theory of monopole condensation.** The monopole interaction in the confinement phase selects

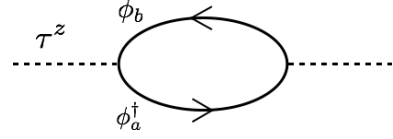


FIG. 4. The bubble diagram of the “magnetic monopole”.

twelve equivalent monopole condensates that correspond to twelve symmetry equivalent Ising orders. In the vicinity of the monopole condensation transition, the monopole condensate and the gauge fields fluctuate strongly. We thereby carry out a Landau-Ginzburg-Wilson expansion of the action in terms of the monopole condensate and gauge field in the vicinity of the phase transition. We introduce the slowly-varying monopole fields  $\phi_a$  via the expansion

$$\Phi_{\mathbf{r}} = \sum_{a=1}^{12} \varphi_a(\mathbf{r}) \phi_a, \quad (18)$$

where  $\varphi_a(\mathbf{r})$  ( $a = 1, \dots, 12$ ) are the twelve discrete monopole modes that span the ground state manifold of the monopole condensate. With the monopole PSG, we generate the symmetry allowed effective action for the monopole condensation transition,

$$L = \sum_a [ |(\partial_\mu - i\tilde{a}_\mu)\phi_a|^2 + m^2|\phi_a|^2 ] + \frac{F_{\mu\nu}^2}{2} + u_0 \left( \sum_a |\phi_a|^2 \right)^2 + u_1 \sum_{a \neq b} |\phi_a|^2 |\phi_b|^2 + \dots, \quad (19)$$

where we have restored the gauge field fluctuation by coupling the  $\phi_a$  fields to the fluctuating part of the dual U(1) gauge field  $\tilde{a}_\mu$ ,  $\frac{1}{2}F_{\mu\nu}^2$  is the Maxwell term with  $F_{\mu\nu} \equiv \partial_\mu \tilde{a}_\nu - \partial_\nu \tilde{a}_\mu$ , “...” contains further anisotropic terms that are marginal for the critical properties,  $m$  is the mass of the monopole and is set by the band gap of the monopole band structure. The effective action in Eq. (19) is a standard multi-component Ginzburg-Landau theory in 3+1D that is the upper critical dimension of the theory. One expects the phase transition of this theory to be governed by a Gaussian fixed point or belong to a weakly first order transition driven by fluctuations<sup>51–53,56,57</sup>. Both possibilities suggest that the mean-field treatment of the phase transition should be sufficient for a rather wide range of length scales. In a mean-field description, the monopole field correlator at the critical point (with the monopole mass  $m = 0$ ) is

$$\langle \phi_a^\dagger(\mathbf{k}, \omega) \phi_b(\mathbf{k}, \omega) \rangle \sim \frac{\delta_{ab}}{\mathbf{k}^2 + \omega^2}. \quad (20)$$

According to Eq. (17), the spin susceptibility at the ordering wavevector  $\mathbf{Q}$  is simply given by the bubble diagram of monopole fields (see Fig. 3) and is thus logarithmically divergent at low temperatures with

$$\chi(\mathbf{Q}) \sim \ln \frac{1}{T}. \quad (21)$$

Such a weak divergence is a unique property of the monopole condensation transition that is a non-Landau-Ginzburg-Wilson transition. For a conventional magnetic transition, one would instead have a power-law divergence for the corresponding susceptibility. Here, the Ising order is a consequence of the monopole condensation. The condensed monopole is the primary order, and the induced Ising order is secondary and is thus a perfect example of the subsidiary order<sup>58,59</sup>.

The monopole mass controls the phase transition and is parameterized as the parameter  $g$  with  $g \equiv -m^2$  in Fig. 1. In the QSI U(1) QSL phase, the monopole is massive with  $m^2 > 0$ . The low energy physics is then governed by the Maxwell's field theory and the emergent gapless gauge photon. Due to the gapless photon, the heat capacity of the system behaves as  $C_v \sim T^3$  at low temperatures. As the system approaches the transition from the QSL side, the monopole mass decreases. The gapless monopole at the criticality gives an extra  $T^3$  contribution to the heat capacity. Therefore, one would observe an enhancement of the  $T^3$  heat capacity as the system approaches the criticality. Moreover, if one raises temperatures in the U(1) QSL side, the generic argument suggests that there is no thermal phase transition except a crossover due to the thermal population of the "magnetic monopoles". The populated monopoles simply create thermal confinement of the spinons at finite temperatures. This crossover temperature is set by the mass of the monopoles.

When  $m^2 < 0$ , the monopole is condensed and the system develops Ising orders. Since the system breaks time reversal symmetry on the ordered side, we should have a finite temperature phase transition above which the time reversal symmetry is restored. The ordering temperature is also set by the mass of the monopoles.

## Discussion.

**The transition and the Ising order in  $\text{Pr}_2\text{Ir}_2\text{O}_7$ .** In  $\text{Pr}_2\text{Ir}_2\text{O}_7$ , the  $\text{Pr}^{3+}$  ion has a  $4f^2$  electron configuration and form a non-Kramers' doublet which is represented by a pseudospin-1/2 operator  $\tau$  with  $\tau^z$  ( $\tau^x, \tau^y$ ) odd (even) under time reversal  $\mathcal{T}$ ,

$$\mathcal{T}: \tau^z \rightarrow -\tau^z, \quad (22)$$

$$\mathcal{T}: \tau^{x,y} \rightarrow \tau^{x,y}. \quad (23)$$

In the disordered state, a metamagnetic transition is observed *only* for magnetic fields along the  $\langle 111 \rangle$  direction. This is a clear evidence that the disordered state of the Pr moments is fluctuating within the ice manifold<sup>12</sup> and the metamagnetic transition is a transition from the "2-in 2-out" ice manifold to the "3-in 1-out" manifold. Since the local moments in QSI U(1) QSL are fluctuating quantum mechanically within the ice manifold, this metamagnetic transition in  $\text{Pr}_2\text{Ir}_2\text{O}_7$  is consistent with our proposal that the disordered state of the Pr moments is a QSI U(1) QSL.

Given the non-Kramers' nature of the Pr moment and its unique time reversal symmetry properties in Eqs. (22)

and (23), the magnetic order of the Pr moment must be the Ising order with  $\langle \tau^z \rangle \neq 0$ . If a non-Kramers doublet local moment system has a QSI U(1) QSL ground state, the magnetic transition from this state *must* be the confinement transition of the compact U(1) LGT because a nonzero  $\tau^z$  corresponds to the static electric field distribution. Remarkably, the Ising order that is found in the ordered  $\text{Pr}_2\text{Ir}_2\text{O}_7$  samples<sup>13</sup> has an ordering wavevector  $\mathbf{Q} = 2\pi(001)$ , and this is precisely the proximate Ising state that we predict from the confinement transition. This experimental result further supports our proposal that the disordered state of the Pr moments in  $\text{Pr}_2\text{Ir}_2\text{O}_7$  is a QSI U(1) QSL.

In different samples, different oxygen and Ir contents shift the Fermi energy of the Ir conduction electrons and thus modify the Ruderman-Kittel-Kasuya-Yosida (RKKY) interaction between the Pr local moments<sup>7,17,60</sup>. This is likely to be the microscopic origin of the sample dependence. Usually the presence of the conduction electron Fermi surface modifies the critical properties of the local moment transition. But  $\text{Pr}_2\text{Ir}_2\text{O}_7$  is very special. Due to the quadratic band touching of the Ir electrons<sup>4,61</sup>, the Fermi energy is very close to the band touching energy and the Fermi momentum  $|\mathbf{k}_F|$  is much smaller than the wavevector  $\mathbf{Q}$  of the magnetic order. As a result, the particle-hole excitations of the Ir system actually decouple from the spin fluctuations of the Pr local moments at low energies<sup>62</sup>. Therefore, the critical properties of the Pr local moments are not modified by the conduction electrons.

At this stage, it is not clear how close the existing  $\text{Pr}_2\text{Ir}_2\text{O}_7$  samples are near the phase transition, therefore, it would be interesting to vary the Ir and/or oxygen contents in a continuous fashion, to drive the system between disordered and ordered phases and directly probe the phase transition. It is very useful to focus on the disordered  $\text{Pr}_2\text{Ir}_2\text{O}_7$  samples and carry out the inelastic neutron scattering. Due to the unique time reversal symmetry properties in Eqs. (22) and (23), only the Ising component of Pr local moment couples with the neutron spin. As the  $\tau^z$  is identified as the emergent electric field, the inelastic neutron scattering directly probes the gauge phonon excitation. Because of the quadratic band touching, the inelastic neutron spectral intensity corresponding to the particle-hole excitations of the Ir electrons concentrate near the  $\Gamma$  point at low energies, and it does not mix with the gauge phonon modes that are peaked near the "pinch point" momenta<sup>29,39</sup>.

**The transition and the magnetic order in  $\text{Yb}_2\text{Ti}_2\text{O}_7$ .** The magnetic state in the ordered  $\text{Yb}_2\text{Ti}_2\text{O}_7$  samples has a  $\mathbf{Q} = (000)$  ferromagnetic order and preserves the translation symmetry<sup>25,43-45</sup>, though many early experiments found a disordered state<sup>23,42</sup>. The thermal transition from the high-temperature paramagnet to the ferromagnetic one is strongly first order<sup>25,44,45</sup>. Unlike the  $\text{Pr}^{3+}$  moment, the  $\text{Yb}^{3+}$  moment is a Kramers' doublet with all pseudospin components odd under time reversal,

thus a direct coupling between  $\tau^z$  and  $\tau^{x,y}$  is allowed. The magnetic transition out of the QSI U(1) QSL for the Kramers' doublet can be either an Anderson-Higgs' transition<sup>25,39,63</sup> or a confinement transition.

In the Higgs' transition scenario<sup>25,39,63</sup>, a predominant transverse component is induced at the first order transition<sup>63</sup>, and a small Ising component is induced simultaneously via the coupling between  $\tau^z$  and  $\tau^{x,y}$ . In the scenario of a confinement transition, however, a predominant Ising order is expected, and this seems to be case in  $\text{Yb}_2\text{Ti}_2\text{O}_7$ <sup>25,44,45</sup>. Moreover, as we have explained, the  $\mathbf{Q} = (000)$  Ising order is not proximate to the QSI U(1) QSL, and the direct transition between them through monopole condensation must be strongly first order. The strongly first order thermal transition in the ordered  $\text{Yb}_2\text{Ti}_2\text{O}_7$  samples can thus be naturally regarded as a finite temperature extension of the zero-temperature one. To differentiate the Higgs' and confinement scenarios in  $\text{Yb}_2\text{Ti}_2\text{O}_7$ , it might be helpful to numerically study the microscopic model<sup>23</sup> by varying the transverse component interaction and the Ising component interaction separately and probe the nature of transition out of the QSI U(1) QSL.

**Summary.** To summarize, we have studied the Ising magnetic orders out of the QSI U(1) QSL via the “magnetic monopole” condensation. We find that such a confinement transition gives rise to the proximate Ising ordered state that breaks the translation symmetry. We propose that the puzzling magnetic properties of  $\text{Pr}_2\text{Ir}_2\text{O}_7$  and  $\text{Yb}_2\text{Ti}_2\text{O}_7$  can be understood from the “magnetic monopole” condensation. Beyond these two systems, we have argued that the magnetic transition out of the QSI U(1) QSL for a non-Kramers doublet local moments must be a confinement transition via monopole condensation. Since the  $\text{Tb}^{3+}$  local moment in  $\text{Tb}_2\text{Ti}_2\text{O}_7$  is a non-Kramers' doublet, it is likely that the sample dependent magnetic order in  $\text{Tb}_2\text{Ti}_2\text{O}_7$ <sup>64</sup> can be understood as the monopole condensation.

## Method.

**Pyrochlore and dual diamond lattices.** Pyrochlore lattice is a corner-shared tetrahedral structure in three dimensions. The centers of the tetrahedra in the pyrochlore lattice form a diamond lattice. The dual lattice of the diamond lattice is also a diamond lattice. For the dual diamond lattice, we choose the sites

$$\mathbf{d}_1 = (0, 0, 0), \quad (24)$$

$$\mathbf{d}_2 = \frac{1}{4}(1, 1, 1), \quad (25)$$

to be the reference points of the I and II sublattices, respectively. The three lattice vectors of the underlying

Bravais lattice are

$$\mathbf{a}_1 = \frac{1}{2}(0, 1, 1), \quad (26)$$

$$\mathbf{a}_2 = \frac{1}{2}(1, 0, 1), \quad (27)$$

$$\mathbf{a}_3 = \frac{1}{2}(1, 1, 0), \quad (28)$$

where we have set the lattice constant to unity.

Each site of the dual diamond lattice is connected by four nearest neighbors. The four vectors  $\mathbf{e}_\mu$  that connect the neighboring sites are given as

$$\mathbf{e}_0 = \frac{1}{4}(1, 1, 1), \quad (29)$$

$$\mathbf{e}_1 = \frac{1}{4}(1, -1, -1), \quad (30)$$

$$\mathbf{e}_2 = \frac{1}{4}(-1, 1, -1), \quad (31)$$

$$\mathbf{e}_3 = \frac{1}{4}(-1, -1, 1). \quad (32)$$

**Projective symmetry group.** Both the pyrochlore lattice and the dual diamond lattice share the same space group symmetry  $\text{Fd}\bar{3}\text{m}$ . The  $\text{Fd}\bar{3}\text{m}$  space group involves three lattice translations,

$$\mathbf{T}_i : \mathbf{r} \rightarrow \mathbf{r} + \mathbf{a}_i, \quad (33)$$

a three-fold rotation,

$$\mathbf{C}_3 : (x, y, z) \rightarrow (z, x, y), \quad (34)$$

a two-fold rotation,

$$\mathbf{C}_2 : (x, y, z) \rightarrow (-x, -y, z), \quad (35)$$

a mirror reflection,

$$\mathbf{R} : (x, y, z) \rightarrow (y, x, z), \quad (36)$$

and an inversion,

$$\mathbf{I} : (x, y, z) \rightarrow \left(\frac{1}{4} - x, \frac{1}{4} - y, \frac{1}{4} - z\right). \quad (37)$$

The physical spin is defined on the pyrochlore lattice site, while the “magnetic monopoles” are defined on the dual diamond lattice sites. Due to the background gauge flux, the space group symmetry is realized projectively in the monopole hopping Hamiltonian  $H_m$ . For each symmetry operation, we need to supplement with a U(1) gauge transformation. Under the symmetry operation  $\hat{O}$ , the monopole is transformed as

$$\hat{O} : \Phi_{\mathbf{r}} \rightarrow e^{-i\Theta_{\mathbf{O}}(\mathbf{r})} \Phi_{\mathbf{r}'}, \quad (38)$$

where  $\mathbf{r}' = \mathbf{O}(\mathbf{r})$  and  $e^{-i\Theta_{\mathbf{O}}(\mathbf{r})}$  is the associated U(1) gauge transformation. We have used  $\hat{O}$  to label the generator of the projective symmetry group.

For our convenience, we introduce the unit cell index  $\mathbf{n}$  to label the monopole position and define

$$\eta_1(\mathbf{n}) = \Phi_{\mathbf{r}}, \quad \eta_2(\mathbf{n}) = \Phi_{\mathbf{r}+\mathbf{e}_0}, \quad (39)$$

where  $\mathbf{r} = \sum_j \mathbf{n}_j \mathbf{a}_j$ , and  $\eta_1(\mathbf{n})$  and  $\eta_2(\mathbf{n})$  are monopole operators on the I and II sublattices, respectively.

Here we list the projective symmetry transformation of the monopole operators. Under the three lattice translations, the monopole operators are transformed as

$$\hat{T}_1 : \eta_1(\mathbf{n}_x, \mathbf{n}_y, \mathbf{n}_z) \rightarrow e^{-i\Theta_{T_1}[\mathbf{n}]} \eta_1(\mathbf{n}_x + 1, \mathbf{n}_y, \mathbf{n}_z), \quad (40)$$

$$\hat{T}_1 : \eta_2(\mathbf{n}_x, \mathbf{n}_y, \mathbf{n}_z) \rightarrow e^{-i\Theta_{T_1}[\mathbf{n}]} \eta_2(\mathbf{n}_x + 1, \mathbf{n}_y, \mathbf{n}_z), \quad (41)$$

$$\hat{T}_2 : \eta_1(\mathbf{n}_x, \mathbf{n}_y, \mathbf{n}_z) \rightarrow e^{-i\Theta_{T_2}[\mathbf{n}]} \eta_1(\mathbf{n}_x, \mathbf{n}_y + 1, \mathbf{n}_z), \quad (42)$$

$$\hat{T}_2 : \eta_2(\mathbf{n}_x, \mathbf{n}_y, \mathbf{n}_z) \rightarrow e^{-i\Theta_{T_2}[\mathbf{n}]} \eta_2(\mathbf{n}_x, \mathbf{n}_y + 1, \mathbf{n}_z), \quad (43)$$

$$\hat{T}_3 : \eta_1(\mathbf{n}_x, \mathbf{n}_y, \mathbf{n}_z) \rightarrow e^{-i\Theta_{T_3}[\mathbf{n}]} \eta_1(\mathbf{n}_x, \mathbf{n}_y, \mathbf{n}_z + 1), \quad (44)$$

$$\hat{T}_3 : \eta_2(\mathbf{n}_x, \mathbf{n}_y, \mathbf{n}_z) \rightarrow e^{-i\Theta_{T_3}[\mathbf{n}]} \eta_2(\mathbf{n}_x, \mathbf{n}_y, \mathbf{n}_z + 1), \quad (45)$$

where

$$\Theta_{T_i}[\mathbf{n}] = -(\boldsymbol{\epsilon} \cdot \mathbf{n}) \mathbf{v}_i \quad (46)$$

and  $\boldsymbol{\epsilon} = (1, 1, 0)$ ,  $\mathbf{v} = \pi(0, 1, 1)$ .

Under three-fold rotation, we have

$$\hat{C}_3 : \eta_1(\mathbf{n}_x, \mathbf{n}_y, \mathbf{n}_z) \rightarrow e^{-i\Theta_{C_3}[\mathbf{n}]} \eta_1(\mathbf{n}_z, \mathbf{n}_x, \mathbf{n}_y), \quad (47)$$

$$\hat{C}_3 : \eta_2(\mathbf{n}_x, \mathbf{n}_y, \mathbf{n}_z) \rightarrow e^{-i\Theta_{C_3}[\mathbf{n}]} \eta_2(\mathbf{n}_z, \mathbf{n}_x, \mathbf{n}_y), \quad (48)$$

where

$$\Theta_{C_3}[\mathbf{n}] = \mathbf{n} \cdot \mathcal{B} \cdot \mathbf{n} + \boldsymbol{\delta} \cdot \mathbf{n} \quad (49)$$

with

$$\mathcal{B} = \frac{\pi}{2} \begin{bmatrix} 1 & 0 & 1 \\ 0 & 1 & 1 \\ 1 & 1 & 0 \end{bmatrix} \quad (50)$$

and  $\boldsymbol{\delta} = \pi/2(1, 1, 0)$ .

Under two-fold rotation, we have

$$\hat{C}_2 : \eta_1(\mathbf{n}_x, \mathbf{n}_y, \mathbf{n}_z) \rightarrow \eta_1(\mathbf{n}_y, \mathbf{n}_x, -\mathbf{n}_x - \mathbf{n}_y - \mathbf{n}_z), \quad (51)$$

$$\hat{C}_2 : \eta_2(\mathbf{n}_x, \mathbf{n}_y, \mathbf{n}_z) \rightarrow \eta_2(\mathbf{n}_y, \mathbf{n}_x, -1 - \mathbf{n}_x - \mathbf{n}_y - \mathbf{n}_z), \quad (52)$$

where  $\Theta_{C_2}[\mathbf{n}] = 0$ .

Under the reflection, we have

$$\hat{R} : \eta_1(\mathbf{n}_x, \mathbf{n}_y, \mathbf{n}_z) \rightarrow e^{-i\Theta_R[\mathbf{n}]} \eta_1(\mathbf{n}_y, \mathbf{n}_x, \mathbf{n}_z), \quad (53)$$

$$\hat{R} : \eta_2(\mathbf{n}_x, \mathbf{n}_y, \mathbf{n}_z) \rightarrow e^{-i\Theta_R[\mathbf{n}]} \eta_2(\mathbf{n}_y, \mathbf{n}_x, \mathbf{n}_z), \quad (54)$$

where

$$\Theta_R[\mathbf{n}] = \mathbf{n} \cdot \mathcal{B}' \cdot \mathbf{n} + \boldsymbol{\delta}' \cdot \mathbf{n} \quad (55)$$

with

$$\mathcal{B}' = \frac{\pi}{2} \begin{bmatrix} 1 & 1 & 0 \\ 1 & 1 & 0 \\ 0 & 0 & 0 \end{bmatrix} \quad (56)$$

and  $\boldsymbol{\delta}' = \pi/2(1, 1, 0)$ .

Finally, for the inversion symmetry, we have

$$\hat{I} : \eta_1(\mathbf{n}_x, \mathbf{n}_y, \mathbf{n}_z) \rightarrow e^{-i\Theta_I[\mathbf{n}]} \eta_2(-\mathbf{n}_x, -\mathbf{n}_y, -\mathbf{n}_z), \quad (57)$$

$$\hat{I} : \eta_2(\mathbf{n}_x, \mathbf{n}_y, \mathbf{n}_z) \rightarrow e^{-i\Theta_I[\mathbf{n}]} \eta_1(-\mathbf{n}_x, -\mathbf{n}_y, -\mathbf{n}_z), \quad (58)$$

where

$$\Theta_I[\mathbf{n}] = \boldsymbol{\lambda} \cdot \mathbf{n} \quad (59)$$

and  $\boldsymbol{\lambda} = \pi(0, 1, 0)$ .

**Further neighbor monopole hoppings.** The general monopole hopping model should be invariant under the PSG transformation. We here give an example for the second neighbor monopole hopping to illustrate the procedure to determine the hopping parameters. The second neighbor connects the lattice sites within the same sublattice. Each site has twelve second-neighbor sites. For the sites in the I sublattice, we consider the monopole hopping Hamiltonian,

$$\begin{aligned} H'_m = & \sum_{\mathbf{n}} d_1[\mathbf{n}] \eta_1^\dagger(\mathbf{n}_x, \mathbf{n}_y, \mathbf{n}_z) \eta_1(\mathbf{n}_x + 1, \mathbf{n}_y, \mathbf{n}_z) \\ & + d_2[\mathbf{n}] \eta_1^\dagger(\mathbf{n}_x, \mathbf{n}_y, \mathbf{n}_z) \eta_1(\mathbf{n}_x, \mathbf{n}_y + 1, \mathbf{n}_z) \\ & + d_3[\mathbf{n}] \eta_1^\dagger(\mathbf{n}_x, \mathbf{n}_y, \mathbf{n}_z) \eta_1(\mathbf{n}_x, \mathbf{n}_y, \mathbf{n}_z + 1) \\ & + d_4[\mathbf{n}] \eta_1^\dagger(\mathbf{n}_x, \mathbf{n}_y, \mathbf{n}_z) \eta_1(\mathbf{n}_x, \mathbf{n}_y - 1, \mathbf{n}_z + 1) \\ & + d_5[\mathbf{n}] \eta_1^\dagger(\mathbf{n}_x, \mathbf{n}_y, \mathbf{n}_z) \eta_1(\mathbf{n}_x - 1, \mathbf{n}_y, \mathbf{n}_z + 1) \\ & + d_6[\mathbf{n}] \eta_1^\dagger(\mathbf{n}_x, \mathbf{n}_y, \mathbf{n}_z) \eta_1(\mathbf{n}_x, \mathbf{n}_y - 1, \mathbf{n}_z + 1) \\ & + h.c., \end{aligned} \quad (60)$$

where  $\{d_i[\mathbf{n}]\}$  are the hopping parameters. Applying the  $\hat{T}_1$  translation, we compare the transformed Hamiltonian with the original Hamiltonian and obtain

$$d_i[\mathbf{n}_x, \mathbf{n}_y, \mathbf{n}_z] = d_i[\mathbf{n}_x - 1, \mathbf{n}_y, \mathbf{n}_z]. \quad (61)$$

Similarly, for the  $\hat{T}_2$  and  $\hat{T}_3$  translations, we have

$$d_1[\mathbf{n}_x, \mathbf{n}_y, \mathbf{n}_z] = -d_1[\mathbf{n}_x, \mathbf{n}_y - 1, \mathbf{n}_z], \quad (62)$$

$$d_2[\mathbf{n}_x, \mathbf{n}_y, \mathbf{n}_z] = -d_2[\mathbf{n}_x, \mathbf{n}_y - 1, \mathbf{n}_z], \quad (63)$$

$$d_3[\mathbf{n}_x, \mathbf{n}_y, \mathbf{n}_z] = +d_3[\mathbf{n}_x, \mathbf{n}_y - 1, \mathbf{n}_z], \quad (64)$$

$$d_4[\mathbf{n}_x, \mathbf{n}_y, \mathbf{n}_z] = -d_4[\mathbf{n}_x, \mathbf{n}_y - 1, \mathbf{n}_z], \quad (65)$$

$$d_5[\mathbf{n}_x, \mathbf{n}_y, \mathbf{n}_z] = -d_5[\mathbf{n}_x, \mathbf{n}_y - 1, \mathbf{n}_z], \quad (66)$$

$$d_6[\mathbf{n}_x, \mathbf{n}_y, \mathbf{n}_z] = +d_6[\mathbf{n}_x, \mathbf{n}_y - 1, \mathbf{n}_z], \quad (67)$$

and

$$d_1[\mathbf{n}_x, \mathbf{n}_y, \mathbf{n}_z] = -d_1[\mathbf{n}_x, \mathbf{n}_y, \mathbf{n}_z - 1], \quad (68)$$

$$d_2[\mathbf{n}_x, \mathbf{n}_y, \mathbf{n}_z] = -d_2[\mathbf{n}_x, \mathbf{n}_y, \mathbf{n}_z - 1], \quad (69)$$

$$d_3[\mathbf{n}_x, \mathbf{n}_y, \mathbf{n}_z] = +d_3[\mathbf{n}_x, \mathbf{n}_y, \mathbf{n}_z - 1], \quad (70)$$

$$d_4[\mathbf{n}_x, \mathbf{n}_y, \mathbf{n}_z] = -d_4[\mathbf{n}_x, \mathbf{n}_y, \mathbf{n}_z - 1], \quad (71)$$

$$d_5[\mathbf{n}_x, \mathbf{n}_y, \mathbf{n}_z] = -d_5[\mathbf{n}_x, \mathbf{n}_y, \mathbf{n}_z - 1], \quad (72)$$

$$d_6[\mathbf{n}_x, \mathbf{n}_y, \mathbf{n}_z] = +d_6[\mathbf{n}_x, \mathbf{n}_y, \mathbf{n}_z - 1], \quad (73)$$

respectively. Applying the remaining symmetries, we obtain the following hopping parameters for the second



neighbors,

$$d_1[n_x, n_y, n_z] = (-)^{n_y+n_z}t_2, \quad (74)$$

$$d_2[n_x, n_y, n_z] = -(-)^{n_y+n_z}t_2, \quad (75)$$

$$d_3[n_x, n_y, n_z] = t_2, \quad (76)$$

$$d_4[n_x, n_y, n_z] = (-)^{n_y+n_z}t_2, \quad (77)$$

$$d_5[n_x, n_y, n_z] = (-)^{n_y+n_z}t_2, \quad (78)$$

$$d_6[n_x, n_y, n_z] = -t_2. \quad (79)$$

With the above procedure, we proceed to generate the further neighbor monopole hoppings up to the fifth neighbors.

**Monopole condensates.** We consider the nearest neighbor monopole hopping model. Due to the background flux and the gauge choice, the unit cell is fictitiously doubled. In Fig. 3, we specify the signs of the hopping parameters on the dual diamond lattice. The lowest energy spectrum has line degeneracies in the momentum space. Focusing on the [001] direction in the momentum space, we have the following eigenstates for a given  $\mathbf{k}_z$ ,

$$\mathbf{r} \in \text{I}, \quad \Phi(\mathbf{r}) = \frac{1}{\sqrt{2}}(e^{i\frac{\mathbf{k}_z}{4}} + e^{-i\frac{\mathbf{k}_z}{4}}e^{i2\pi x})e^{ik_z z}, \quad (80)$$

$$\mathbf{r} \in \text{II}, \quad \Phi(\mathbf{r}) = e^{ik_z z}. \quad (81)$$

The monopoles are condensed at these lowest energy momenta. To satisfy the unimodular condition for the monopoles, we immediately require the monopoles to be condensed at  $\mathbf{k}_z = \pm\pi$ .

**A sign-problem free model for quantum Monte Carlo simulation.** Here we propose a simple exchange model that does not have a sign problem for quantum Monte Carlo (QMC) simulation. This model can realize both the  $\mathbf{Q} = 2\pi(001)$  order and the  $\mathbf{Q} = (000)$  order. Although both Ising orders belong to the spin ice manifold, the former is proximate to the QSI U(1) QSL via a confinement transition and the latter is not (see the main text for the detailed discussion). The model is given as

$$H_1 = \sum_{\langle ij \rangle} J_z \tau_i^z \tau_j^z - J_\perp (\tau_i^+ \tau_j^- + h.c.) + \sum_{\langle\langle ij \rangle\rangle} J_{3z} \tau_i^z \tau_j^z, \quad (82)$$

where  $J_{3z}$  is the third neighbor Ising exchange.

We focus our discussion on the case when  $J_\perp > 0$ . This is precisely the parameter regime where the sign problem for QMC is absent. To be in the spin ice regime, we keep

$J_z > 0$ . When  $J_\pm \ll J_z$  and  $J_{3z} \ll J_z$ , the ground state is a QSI U(1) QSL. If we fix  $J_\pm/J_z$  to make the system in the QSI U(1) QSL phase, as we gradually increase  $|J_{3z}/J_z|$  from 0, the system will eventually become ordered. Since  $J_{3z}$  is the interaction between spins from the same sublattice, a ferromagnetic  $J_{3z}$  would simply favor  $\mathbf{Q} = (000)$ , even though the four spins on each tetrahedron of the pyrochlore lattice obey the “two-in two-out” ice rule (see Fig. 2a of the main text). Since this  $\mathbf{Q} = (000)$  is not proximate to the U(1) QSL phase, we expect a *strongly first order* transition as we increase  $|J_{3z}/J_z|$  for a ferromagnetic  $J_{3z}$ .

For an antiferromagnetic  $J_{3z}$ , although the Luttinger-Tisza method gives a continuous line degeneracy for the ordering wavevector, the Ising constraint immediately select the collinear order with an ordering wavevector  $\mathbf{Q} = 2\pi(001)$ . As we show in the main text, this Ising order is proximate to the U(1) QSL via a monopole condensation transition. Therefore, we expect either a continuous transition or an extremely weakly first order transition driven by fluctuations as we increase  $|J_{3z}/J_z|$  for an antiferromagnetic  $J_{3z}$ .

In the future, it would be interesting to implement a large scale QMC simulation of the model in Eq. (82) to confirm the monopole condensation transition out the QSI U(1) QSL.

Finally, we propose a perturbative version of the model in Eq. (82). The new model includes the ring exchange on the pyrochlore hexagons and the third neighbor Ising exchange and is given as

$$H_2 = - \sum_{\square_p} \frac{K}{2} (\tau_1^+ \tau_2^- \tau_3^+ \tau_4^- \tau_5^+ \tau_6^- + h.c.) + \sum_{\langle\langle ij \rangle\rangle} J_{3z} \tau_i^z \tau_j^z, \quad (83)$$

and we further restrict the Hilbert space to be the “2-in 2-out” ice manifold. Therefore, this new Hamiltonian will only act on the states in the ice manifold. This perturbative model was already proposed in one perturbative limit of the realistic spin model for  $\text{Yb}_2\text{Ti}_2\text{O}_7$  in Ref. 39. When  $|J_{3z}| \ll K$ , the ground state of  $H_2$  is the QSI U(1) QSL phase. When  $|J_{3z}| \gg K$ , the system develops  $\mathbf{Q} = 2\pi(001)$  antiferromagnetic order for a positive  $J_{3z}$ , and  $\mathbf{Q} = (000)$  ferromagnetic order for a negative  $J_{3z}$ . Again, we expect the transition from the QSI U(1) QSL to the ferromagnetic state is strongly first order, while the transition to the antiferromagnetic state is either continuous or extremely weakly first order.

<sup>1</sup> Daiki Yanagishima and Yoshiteru Maeno, “Metal-nonmetal changeover in pyrochlore iridates,” *Journal of the Physical Society of Japan* **70**, 2880–2883 (2001).

<sup>2</sup> Kazuyuki Matsuhira, Makoto Wakeshima, Ryo Nakan-

ishi, Takaaki Yamada, Akira Nakamura, Wataru Kawano, Seishi Takagi, and Yukio Hinatsu, “Metalinsulator transition in pyrochlore iridates  $\text{Ln}_2\text{Ir}_2\text{O}_7$  ( $\text{Ln} = \text{nd, sm, and eu}$ ),” *Journal of the Physical Society of Japan* **76**, 043706



- (2007).
- <sup>3</sup> D. Pesin and L. Balents, “Mott physics and band topology in materials with strong spinorbit interaction,” *Nature Physics* **6**, 376–381 (2010).
  - <sup>4</sup> Bohm-Jung Yang and Yong Baek Kim, “Topological insulators and metal-insulator transition in the pyrochlore iridates,” *Phys. Rev. B* **82**, 085111 (2010).
  - <sup>5</sup> Xiangang Wan, Ari M. Turner, Ashvin Vishwanath, and Sergey Y. Savrasov, “Topological semimetal and fermi-arc surface states in the electronic structure of pyrochlore iridates,” *Phys. Rev. B* **83**, 205101 (2011).
  - <sup>6</sup> William Witczak-Krempa and Yong Baek Kim, “Topological and magnetic phases of interacting electrons in the pyrochlore iridates,” *Phys. Rev. B* **85**, 045124 (2012).
  - <sup>7</sup> Gang Chen and Michael Hermele, “Magnetic orders and topological phases from  $f$ - $d$  exchange in pyrochlore iridates,” *Phys. Rev. B* **86**, 235129 (2012).
  - <sup>8</sup> Eun-Gook Moon, Cenke Xu, Yong Baek Kim, and Leon Balents, “Non-fermi-liquid and topological states with strong spin-orbit coupling,” *Phys. Rev. Lett.* **111**, 206401 (2013).
  - <sup>9</sup> Lucile Savary, Eun-Gook Moon, and Leon Balents, “New type of quantum criticality in the pyrochlore iridates,” *Phys. Rev. X* **4**, 041027 (2014).
  - <sup>10</sup> S. Nakatsuji, Y. Machida, Y. Maeno, T. Tayama, T. Sakakibara, J. van Duijn, L. Balicas, J. N. Millican, R. T. Macaluso, and Julia Y. Chan, “Metallic spin-liquid behavior of the geometrically frustrated kondo lattice  $\text{pr}_2\text{ir}_2\text{o}_7$ ,” *Phys. Rev. Lett.* **96**, 087204 (2006).
  - <sup>11</sup> Y. Machida, S. Nakatsuji, Y. Maeno, T. Tayama, T. Sakakibara, and S. Onoda, “Unconventional anomalous hall effect enhanced by a noncoplanar spin texture in the frustrated kondo lattice  $\text{pr}_2\text{ir}_2\text{o}_7$ ,” *Phys. Rev. Lett.* **98**, 057203 (2007).
  - <sup>12</sup> Y. Machida, S. Nakatsuji, S. Onoda, T. Tayama, and T. Sakakibara, “Time-reversal symmetry breaking and spontaneous hall effect without magnetic dipole order,” *Nature* **463**, 210–213 (2009).
  - <sup>13</sup> D. E. MacLaughlin, O. O. Bernal, Lei Shu, Jun Ishikawa, Yosuke Matsumoto, J.-J. Wen, M. Mourigal, C. Stock, G. Ehlers, C. L. Broholm, Yo Machida, Kenta Kimura, Satoru Nakatsuji, Yasuyuki Shimura, and Toshiro Sakakibara, “Unstable spin-ice order in the stuffed metallic pyrochlore  $\text{pr}_{2+x}\text{ir}_{2-x}\text{o}_{7-\delta}$ ,” *Phys. Rev. B* **92**, 054432 (2015).
  - <sup>14</sup> William Witczak-Krempa, Gang Chen, Yong Baek Kim, and Leon Balents, “Correlated quantum phenomena in the strong spin-orbit regime,” *Annual Review of Condensed Matter Physics* **5**, 57–82 (2014).
  - <sup>15</sup> R. Schaffer, Eric Kin-Ho Lee, Bohm-Jung Yang, and Yong Baek Kim, “Recent progress on correlated electron systems with strong spin-orbit coupling,” *ArXiv:1512.02224* (2015).
  - <sup>16</sup> Rebecca Flint and T. Senthil, “Chiral rkky interaction in  $\text{pr}_2\text{ir}_2\text{o}_7$ ,” *Phys. Rev. B* **87**, 125147 (2013).
  - <sup>17</sup> SungBin Lee, Arun Paramekanti, and Yong Baek Kim, “Rkky interactions and the anomalous hall effect in metallic rare-earth pyrochlores,” *Phys. Rev. Lett.* **111**, 196601 (2013).
  - <sup>18</sup> Zhaoming Tian, Yoshimitsu Kohama, Takahiro Tomita, Hiroaki Ishizuka, Timothy H Hsieh, Jun J Ishikawa, Koichi Kindo, Leon Balents, and Satoru Nakatsuji, “Field-induced quantum metal-insulator transition in the pyrochlore iridate  $\text{nd}_2\text{ir}_2\text{o}_7$ ,” *Nature Physics* (2015).
  - <sup>19</sup> Michael Hermele, Matthew P. A. Fisher, and Leon Balents, “Pyrochlore photons: The  $u(1)$  spin liquid in a  $s = \frac{1}{2}$  three-dimensional frustrated magnet,” *Phys. Rev. B* **69**, 064404 (2004).
  - <sup>20</sup> Hamid R. Molavian, Michel J. P. Gingras, and Benjamin Canals, “Dynamically induced frustration as a route to a quantum spin ice state in  $\text{tb}_2\text{ti}_2\text{o}_7$  via virtual crystal field excitations and quantum many-body effects,” *Phys. Rev. Lett.* **98**, 157204 (2007).
  - <sup>21</sup> David A. Huse, Werner Krauth, R. Moessner, and S. L. Sondhi, “Coulomb and liquid dimer models in three dimensions,” *Phys. Rev. Lett.* **91**, 167004 (2003).
  - <sup>22</sup> Lucile Savary and Leon Balents, “Quantum spin liquids,” *ArXiv:1601.03742* (2016).
  - <sup>23</sup> Kate Ross, Lucile Savary, Bruce Gaulin, and Leon Balents, “Quantum excitations in quantum spin ice,” *Phys. Rev. X* **1**, 021002 (2011).
  - <sup>24</sup> K. Kimura, K. Nakatsuji, J.-J. Wen, C. Broholm, M.B. Stone, E. Nishibori, and H. Sawa, “Quantum fluctuations in spin-ice-like  $\text{pr}_2\text{zr}_2\text{o}_7$ ,” *Nature Communications* **4**, 2914 (2013).
  - <sup>25</sup> Lieh-Jeng Chang, Shigeki Onoda, Yixi Su, Ying-Jer Kao, Ku-Ding Tsuei, Yukio Yasui, Kazuhisa Kakurai, and Martin Richard Lees, “Higgs transition from a magnetic coulomb liquid to a ferromagnet in  $\text{yb}_2\text{ti}_2\text{o}_7$ ,” *Nature Communications* **3**, 992 (2012).
  - <sup>26</sup> Yuan Wan and Oleg Tchernyshyov, “Quantum strings in quantum spin ice,” *Phys. Rev. Lett.* **108**, 247210 (2012).
  - <sup>27</sup> J. S. Gardner, S. R. Dunsiger, B. D. Gaulin, M. J. P. Gingras, J. E. Greedan, R. F. Kiefl, M. D. Lumsden, W. A. MacFarlane, N. P. Raju, J. E. Sonier, I. Swainson, and Z. Tun, “Cooperative paramagnetism in the geometrically frustrated pyrochlore antiferromagnet  $\text{tb}_2\text{ti}_2\text{o}_7$ ,” *Phys. Rev. Lett.* **82**, 1012–1015 (1999).
  - <sup>28</sup> J. S. Gardner, B. D. Gaulin, A. J. Berlinsky, P. Waldron, S. R. Dunsiger, N. P. Raju, and J. E. Greedan, “Neutron scattering studies of the cooperative paramagnet pyrochlore  $\text{tb}_2\text{ti}_2\text{o}_7$ ,” *Phys. Rev. B* **64**, 224416 (2001).
  - <sup>29</sup> Owen Benton, Olga Sikora, and Nic Shannon, “Seeing the light: Experimental signatures of emergent electromagnetism in a quantum spin ice,” *Phys. Rev. B* **86**, 075154 (2012).
  - <sup>30</sup> Yukio Yasui, Masaki Kanada, Masafumi Ito, Hiroshi Harashina, Masatoshi Sato, Hajime Okumura, Kazuhisa Kakurai, and Hiroaki Kadowaki, “Static correlation and dynamical properties of  $\text{tb}_3^{+}$ -moments in  $\text{tb}_2\text{ti}_2\text{o}_7$  neutron scattering study,” *Journal of the Physical Society of Japan* **71**, 599–606 (2002).
  - <sup>31</sup> T. Fennell, M. Kenzelmann, B. Roessli, M. K. Haas, and R. J. Cava, “Power-law spin correlations in the pyrochlore antiferromagnet  $\text{tb}_2\text{ti}_2\text{o}_7$ ,” *Phys. Rev. Lett.* **109**, 017201 (2012).
  - <sup>32</sup> K. C. Rule, J. P. C. Ruff, B. D. Gaulin, S. R. Dunsiger, J. S. Gardner, J. P. Clancy, M. J. Lewis, H. A. Dabkowska, I. Mirebeau, P. Manuel, Y. Qiu, and J. R. D. Copley, “Field-induced order and spin waves in the pyrochlore antiferromagnet  $\text{tb}_2\text{ti}_2\text{o}_7$ ,” *Phys. Rev. Lett.* **96**, 177201 (2006).
  - <sup>33</sup> Steven T. Bramwell and Michel J. P. Gingras, “Spin ice state in frustrated magnetic pyrochlore materials,” *Science* **294**, 1495–1501 (2001).
  - <sup>34</sup> M. J. Harris, S. T. Bramwell, D. F. McMorrow, T. Zeiske, and K. W. Godfrey, “Geometrical frustration in the ferromagnetic pyrochlore  $\text{ho}_2\text{ti}_2\text{o}_7$ ,” *Phys. Rev. Lett.* **79**, 2554–2557 (1997).

- <sup>35</sup> C. Castelnovo<sup>1</sup>, R. Moessner, and S. L. Sondhi, “Magnetic monopoles in spin ice,” *Nature* **451**, 42–45 (2008).
- <sup>36</sup> Jason S. Gardner, Michel J. P. Gingras, and John E. Greedan, “Magnetic pyrochlore oxides,” *Rev. Mod. Phys.* **82**, 53–107 (2010).
- <sup>37</sup> M J P Gingras and P A McClarty, “Quantum spin ice: a search for gapless quantum spin liquids in pyrochlore magnets,” *Reports on Progress in Physics* **77**, 056501 (2014).
- <sup>38</sup> Zhihao Hao, Alexandre G. R. Day, and Michel J. P. Gingras, “Bosonic many-body theory of quantum spin ice,” *Phys. Rev. B* **90**, 214430 (2014).
- <sup>39</sup> Lucile Savary and Leon Balents, *Phys. Rev. Lett.* **108**, 037202 (2012).
- <sup>40</sup> SungBin Lee, Shigeki Onoda, and Leon Balents, “Generic quantum spin ice,” *Phys. Rev. B* **86**, 104412 (2012).
- <sup>41</sup> Yi-Ping Huang, Gang Chen, and Michael Hermele, “Quantum spin ices and topological phases from dipolar-octupolar doublets on the pyrochlore lattice,” *Phys. Rev. Lett.* **112**, 167203 (2014).
- <sup>42</sup> K. A. Ross, J. P. C. Ruff, C. P. Adams, J. S. Gardner, H. A. Dabkowska, Y. Qiu, J. R. D. Copley, and B. D. Gaulin, “Two-dimensional kagome correlations and field induced order in the ferromagnetic  $xy$  pyrochlore  $\text{Yb}_2\text{Ti}_2\text{O}_7$ ,” *Phys. Rev. Lett.* **103**, 227202 (2009).
- <sup>43</sup> Yukio Yasui, Minoru Soda, Satoshi Iikubo, Masafumi Ito, Masatoshi Sato, Nobuko Hamaguchi, Taku Matsushita, Nobuo Wada, Tetsuya Takeuchi, Naofumi Aso, and Kazuhisa Kakurai, “Ferromagnetic transition of pyrochlore compound  $\text{Yb}_2\text{Ti}_2\text{O}_7$ ,” *Journal of the Physical Society of Japan* **72**, 3014–3015 (2003).
- <sup>44</sup> Lieh-Jeng Chang, Martin R. Lees, Isao Watanabe, Adrian D. Hillier, Yukio Yasui, and Shigeki Onoda, “Static magnetic moments revealed by muon spin relaxation and thermodynamic measurements in the quantum spin ice  $\text{Yb}_2\text{Ti}_2\text{O}_7$ ,” *Phys. Rev. B* **89**, 184416 (2014).
- <sup>45</sup> E. Lhotel, S. R. Giblin, M. R. Lees, G. Balakrishnan, L. J. Chang, and Y. Yasui, “First-order magnetic transition in  $\text{Yb}_2\text{Ti}_2\text{O}_7$ ,” *Phys. Rev. B* **89**, 224419 (2014).
- <sup>46</sup> The “magnetic monopole” used here is distinct from the magnetic monopole of Ref. 35. So a quotation mark is used.
- <sup>47</sup> Eduardo Fradkin and Stephen H. Shenker, “Phase diagrams of lattice gauge theories with higgs fields,” *Phys. Rev. D* **19**, 3682–3697 (1979).
- <sup>48</sup> Robert Savit, “Duality in field theory and statistical systems,” *Rev. Mod. Phys.* **52**, 453–487 (1980).
- <sup>49</sup> C. Dasgupta and B. I. Halperin, “Phase transition in a lattice model of superconductivity,” *Phys. Rev. Lett.* **47**, 1556–1560 (1981).
- <sup>50</sup> Michael E Peskin, “Mandelstam-’t hooft duality in abelian lattice models,” *Annals of Physics* **113**, 122 – 152 (1978).
- <sup>51</sup> Doron L. Bergman, Gregory A. Fiete, and Leon Balents, “Ordering in a frustrated pyrochlore antiferromagnet proximate to a spin liquid,” *Phys. Rev. B* **73**, 134402 (2006).
- <sup>52</sup> O. I. Motrunich and T. Senthil, “Origin of artificial electrodynamics in three-dimensional bosonic models,” *Phys. Rev. B* **71**, 125102 (2005).
- <sup>53</sup> Leon Balents and Subir Sachdev, “Dual vortex theory of doped mott insulators,” *Annals of Physics* **322**, 2635 – 2664 (2007).
- <sup>54</sup> Xiao-Gang Wen, “Quantum orders and symmetric spin liquids,” *Phys. Rev. B* **65**, 165113 (2002).
- <sup>55</sup> See the Method for the details.
- <sup>56</sup> B. I. Halperin, T. C. Lubensky, and Shang-keng Ma, “First-order phase transitions in superconductors and smectic- $a$  liquid crystals,” *Phys. Rev. Lett.* **32**, 292–295 (1974).
- <sup>57</sup> Leon Balents, Lorenz Bartosch, Anton Burkov, Subir Sachdev, and Krishnendu Sengupta, “Putting competing orders in their place near the mott transition,” *Phys. Rev. B* **71**, 144508 (2005).
- <sup>58</sup> Erez Berg, Eduardo Fradkin, and Steven A Kivelson, “Charge-4e superconductivity from pair-density-wave order in certain high-temperature superconductors,” *Nature Physics* **5**, 830–833 (2009).
- <sup>59</sup> Patrick A. Lee, “Amperean pairing and the pseudogap phase of cuprate superconductors,” *Phys. Rev. X* **4**, 031017 (2014).
- <sup>60</sup> Yao-Dong Li and Gang Chen, Unpublished (2016).
- <sup>61</sup> Takeshi Kondo, M Nakayama, R Chen, JJ Ishikawa, E-G Moon, T Yamamoto, Y Ota, W Malaeb, H Kanai, Y Nakashima, *et al.*, “Quadratic fermi node in a 3d strongly correlated semimetal,” *Nature communications* **6** (2015).
- <sup>62</sup> Hilbert v. Löhneysen, Achim Rosch, Matthias Vojta, and Peter Wölfle, “Fermi-liquid instabilities at magnetic quantum phase transitions,” *Rev. Mod. Phys.* **79**, 1015–1075 (2007).
- <sup>63</sup> Lucile Savary and Leon Balents, “Spin liquid regimes at nonzero temperature in quantum spin ice,” *Phys. Rev. B* **87**, 205130 (2013).
- <sup>64</sup> K. Fritsch, E. Kermarrec, K. A. Ross, Y. Qiu, J. R. D. Copley, D. Pomaranski, J. B. Kycia, H. A. Dabkowska, and B. D. Gaulin, “Temperature and magnetic field dependence of spin-ice correlations in the pyrochlore magnet  $\text{Yb}_2\text{Ti}_2\text{O}_7$ ,” *Phys. Rev. B* **90**, 014429 (2014).

**Acknowledgements.**—I am particularly indebted to Leon Balents for the clarification of his early work and the encouragement. I am especially grateful to M.P.A. Fisher for his emphasis on universality in a conversation that inspired me significantly. I acknowledge very useful conversation with C. Broholm, J.G. Cheng, X. Dai, G. Fiete, L.Y. Hung, Y.B. Kim, S.S. Lee, S. Nakatsuji, T. Senthil, F. Wang, Z.Y. Weng, F.C. Zhang, and Y. Zhou and an early collaboration with M. Hermele. I sincerely thank the hospitality of Oleg Tchernyshov for inviting me to a pleasant trip at Johns Hopkins University where some of the insights were developed. Finally, I thank the hospitality of Fuchun Zhang and Yi Zhou for supporting my stay at Zhejiang University in April and May 2015 when and where most part of the work was carried out. The work is supported by the starting-up fund of Fudan University (Shanghai, People’s Republic of China) and the Thousand-Youth-Talent Program of People’s Republic of China.

**Additional information** The authors declare no competing financial interests.